Computational Ocean Acoustics

- Ray Tracing
- Wavenumber Integration
- Normal Modes
- Parabolic Equation

Wavenumber Integration

- Range-independent – Integral Transform solution
- Exact depth-dependent solution
  - Global Matrix Approach
  - Propagator Matrix Approach
  - Invariant Embedding
- Numerical Integration
  - Fast-Field Program (FFP)
  - Fast Hankel Transform
- Numerical issues:
  - Numerical stability of depth solution
  - Aliasing and wrap-around

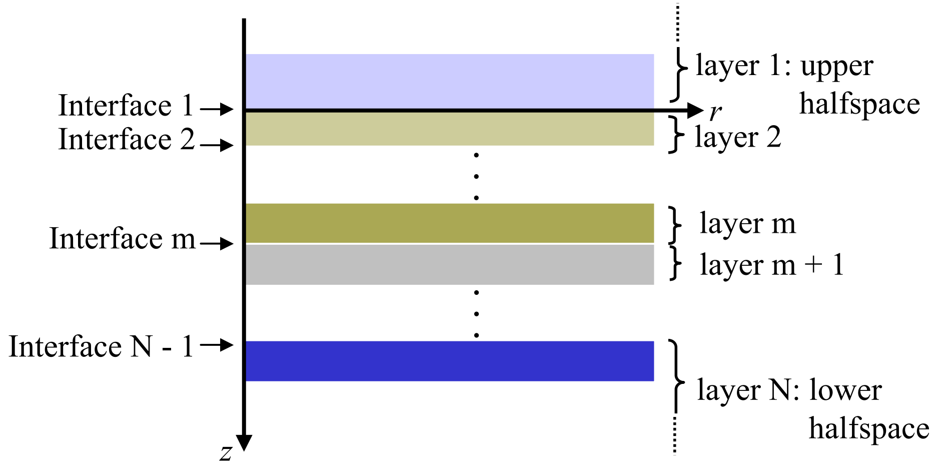

Horiztonally stratified environment

Wavenumber Integration Techniques

Integral Transform Solution

Helmholtz Equation for Displacement Potentials

$$\left[\nabla^2 + k_m^2(z)\right]\psi_m(r,z) \;=\; f_s(z,\omega)\,\frac{\delta(r)}{2\pi r}\;,$$

Medium wavenumber: $$k_m(z) \;=\; \frac{\omega}{c(z)}$$

Hankel Transform Pair

$$f(r,z) = \int_0^\infty f(k_r,z)\, J_0(k_r r)\, k_r\, dk_r \,,$$
$$f(k_r,z) = \int_0^\infty f(r,z)\, J_0(k_r r)\, r\, dr \,,$$

Integral Transform Solution

Depth-separated Wave Equation

$$\left[\frac{d^2}{dz^2} - \left[k_r^2 - k_m^2(z)\right]\right] \psi_m(k_r,z) = \frac{f_s(z)}{2\pi} \,,$$

Superposition Principle

$$\psi_m(k_r,z) = \underbrace{\widehat{\psi}_m(k_r,z)}_{\text{Source}} + \underbrace{A_m^+(k_r)\, \psi_m^+(k_r,z) + A_m^-(k_r)\, \psi_m^-(k_r,z)}_{\text{Homogeneous Solution}} \,,$$

Wavenumber Integration

$$g(r,z) = \int_0^\infty g(k_r,z)\, J_0(k_r r)\, k_r\, dk_r \ ,$$

Complications

- The *infinite* integration interval.
- The *wavenumber discretization* giving rise to *aliasing* and *wrap-around* problems because of the oscillatory nature of the Bessel function, and the variation of the kernel $g(k_r,z)$ which for waveguide problems has poles on or close to the real wavenumber axis.

Fast Field Approximation

$$J_0(k_r r) = \frac{1}{2}\left[H_0^{(1)}(k_r r) + H_0^{(2)}(k_r r)\right] \ ,$$

$$\lim_{Kr\to\infty} H_0^{(1)}(k_r r) = \sqrt{\frac{2}{\pi k_r r}}\, e^{i\left[k_r r - \frac{\pi}{4}\right]} \ ,$$

$$g(r,z) \simeq \sqrt{\frac{1}{2\pi r}}\, e^{-i\frac{\pi}{4}} \int_0^\infty g(k_r,z)\, \sqrt{k_r}\, e^{ik_r r} dk_r \ .$$

Outgoing waves only

Truncation of Integration Interval

$$\psi_m(k_r,z) = \underbrace{\hat{\psi}_m(k_r,z)}_{\text{Source}} + \underbrace{A_m^+(k_r)\,\psi_m^+(k_r,z) + A_m^-(k_r)\,\psi_m^-(k_r,z)}_{\text{Homogeneous Solution}},$$

$$\hat{\phi}(k_r,z) = \frac{S_\omega}{4\pi}\,\frac{e^{ik_z|z-z_s|}}{ik_z},$$

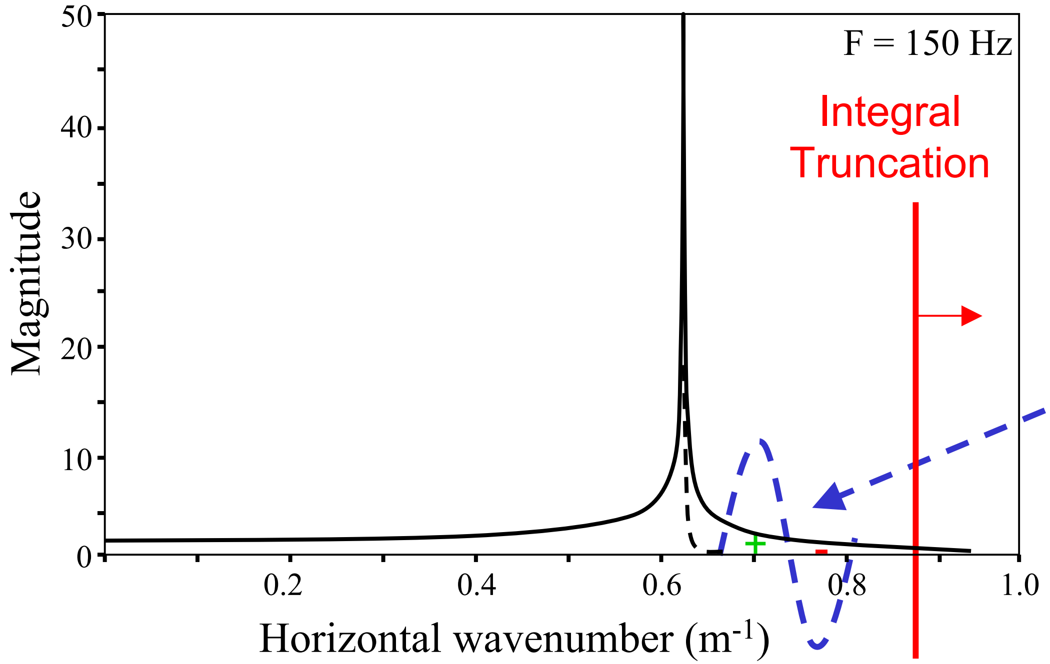

- Slow evanescent decay if receiver depth close to source depth
- Homogeneous solution decay slow if source close to interfaces
- Short range – slow exp() oscillation -> Evanescent contribution significant
- Long range – fast exp() oscillation -> Evanescent contribution insignificant

Truncation of Integration Interval

$$\psi_m(k_r,z) = \underbrace{\hat{\psi}_m(k_r,z)}_{\text{Source}} + \underbrace{A_m^+(k_r)\,\psi_m^+(k_r,z) + A_m^-(k_r)\,\psi_m^-(k_r,z)}_{\text{Homogeneous Solution}},$$

$$\hat{\phi}(k_r,z) = \frac{S_\omega}{4\pi}\,\frac{e^{ik_z|z-z_s|}}{ik_z},$$

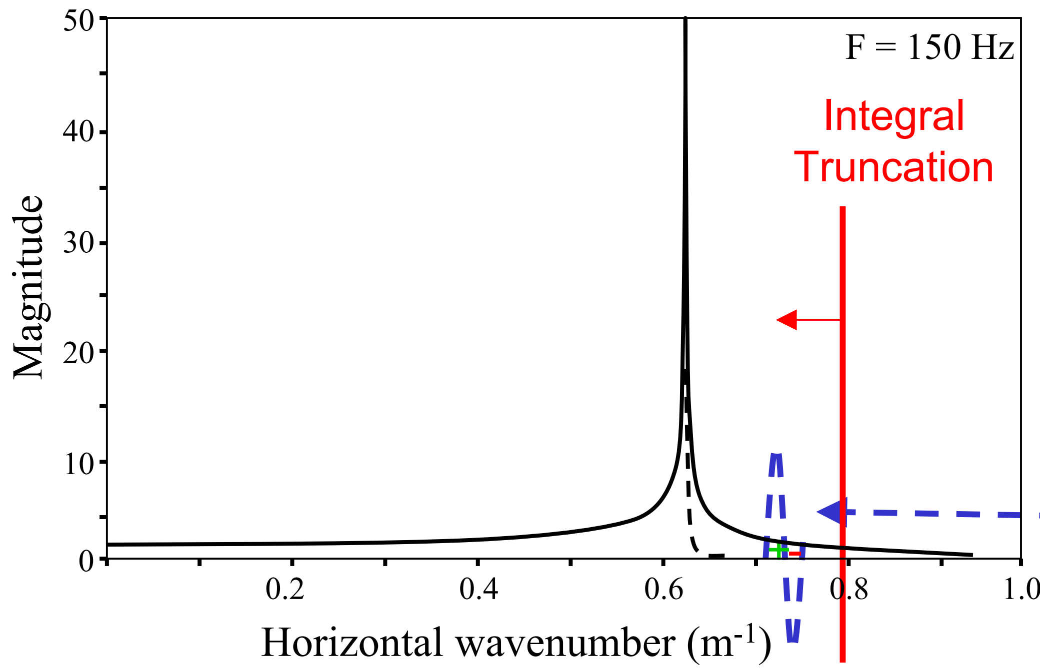

- Slow evanescent decay if receiver depth close to source depth
- Homogeneous solution decay slow if source close to interfaces
- Short range – slow exp() oscillation -> Evanescent contribution significant
- Long range – fast exp() oscillation -> Evanescent contribution insignificant

$$g(r,z) \simeq \sqrt{\frac{1}{2\pi r}}\, e^{-i\frac{\pi}{4}} \int_0^\infty g(k_r,z)\,\sqrt{k_r}\, e^{ik_r r} dk_r \; .$$

Discrete wavenumber sampling

$$k_\ell = k_{\min} + \ell\,\Delta k_r\;, \qquad \ell = 0, 1 \ldots (M-1)\;,$$

$$\Delta k_r = (k_{\max} - k_{\min})/(M-1)$$

Discrete FFP Approximation

$$g^*(r,z) = \frac{\Delta k_r}{\sqrt{2\pi r}}\, e^{i\left[k_{\min} r - \frac{\pi}{4}\right]} \sum_{\ell=0}^{M-1} \left[g(k_\ell,z)\sqrt{k_\ell}\right] e^{i\ell\Delta k_r r}\;,$$

Fast Field Discretization Error?

Range-depth factorization

$$g(r,z) \simeq h(r) f(r,z),$$

Geometric spreading factor

$$h(r) = \sqrt{\frac{1}{2\pi r}}\, e^{-i\frac{\pi}{4}}$$

Wavenumber integral

$$f(r,z) = \int_0^{\infty} g(k_r,z)\, \sqrt{k_r}\, e^{ik_r r} dk_r \; .$$

Discrete factorization

$$g^*(r,z) = h(r) e^{ik_{\min} r} f^*(r,z),$$

$$f^*(r,z) = \Delta k_r \sum_{\ell=0}^{M-1} g(k_\ell, z)\, \sqrt{k_\ell}\, e^{ir\ell\Delta k_r} \; .$$

Periodicity

$$R = \frac{2\pi}{\Delta k_r}$$

$$\begin{aligned} f^*(r+nR,z) &\equiv f^*(r,z),\ n = -\infty, \ldots, 0, \ldots \infty. \\ \frac{\partial^m f^*}{\partial r^m}\Big|_r &= \frac{\partial^m f^*}{\partial r^m}\Big|_{r+nR} \\ &\Rightarrow \\ \frac{\partial^m f^*}{\partial r^m}\Big|_{r_{\min}} &= \frac{\partial^m f^*}{\partial r^m}\Big|_{r_{\min}+nR} \end{aligned}$$

Wrap-around - Aliasing

$$g^*(r,z) = h(r)e^{ik_{\min}r} f^*(r,z) = h(r) \sum_{n=-\infty}^{\infty} f(r+nR,z),$$

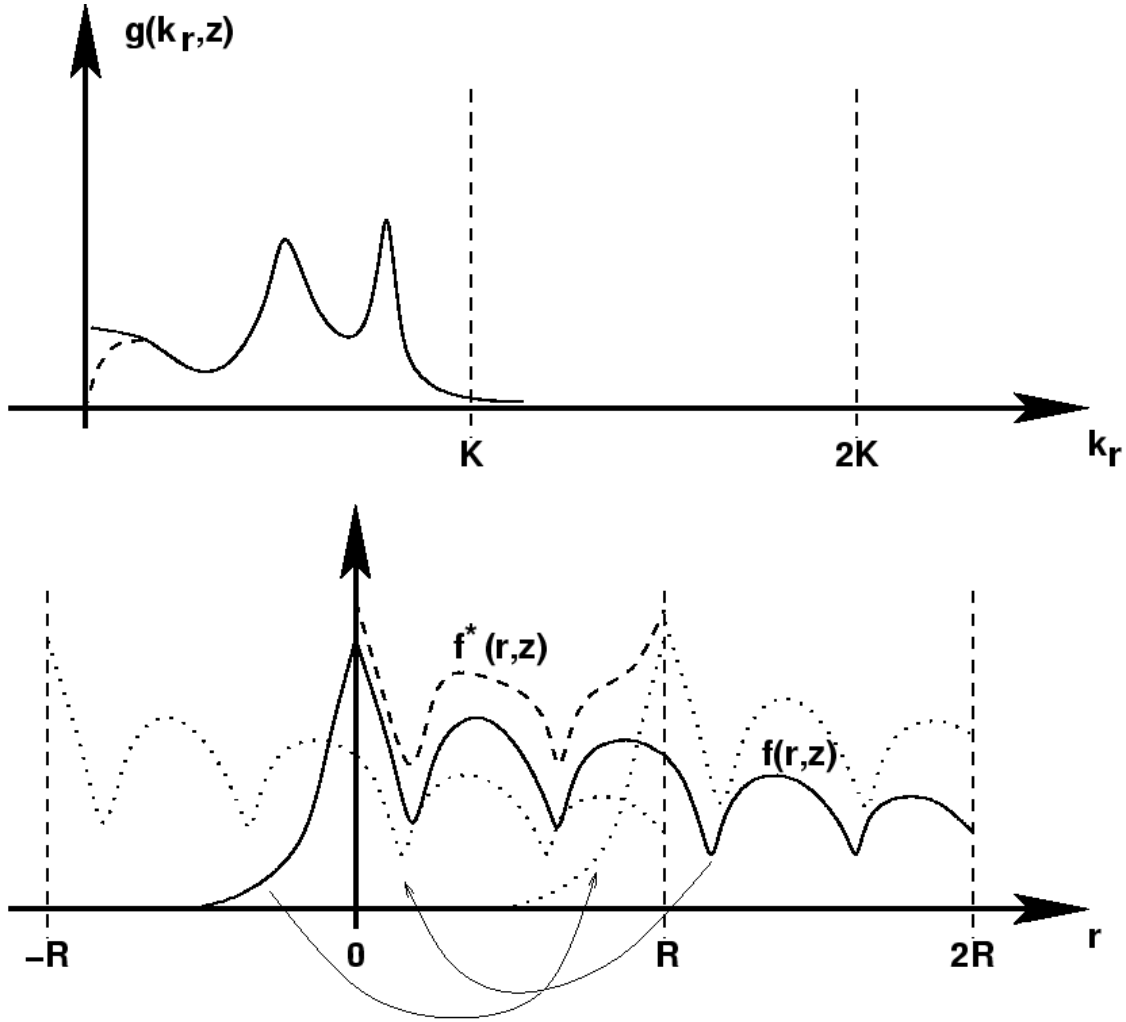

Aliasing associated with discrete wavenumber integration for typical Pekeris waveguide problem. The wavenumber kernel showing the presence of a two attenuated modes is sketched in the upper plot, with the squareroot singularity introduced by the geometric $\sqrt{k_r}$ indicated by the dashed curve near the origin. The discrete wavenumber integration yields the periodic result shown in the lower frame by a dashed curve, approximating the correct continuous result shown as a solid curve. The discrete result is a superposition of the 'true' field produced by the mirror sources in all the range windows.

FFP: Fast Field Program

Range Discretization

$$r_j = r_{\min} + j\,\Delta r\,, \qquad j = 0, 1 \ldots (M-1)\,,$$

$$\Delta r\,\Delta k_r = \frac{2\pi}{M}\,,$$

Discrete Approximation

$$g^*(r_j, z) = \frac{\Delta k_r}{\sqrt{2\pi r_j}}\, e^{i\left[k_{\min} r_j - (m+\frac{1}{2})\frac{\pi}{2}\right]} \sum_{\ell=0}^{M-1} \left[g(k_\ell, z)\, e^{i r_{\min} \ell\,\Delta k_r} \sqrt{k_\ell}\right] e^{i\frac{2\pi \ell j}{M}}\,,$$

Negative Spectrum wrap-around

$$e^{i(-\ell\Delta k_r)(j\Delta r)} = e^{i(2\pi\ \ -\ell\Delta k_r(j\Delta r))} = e^{i(M-\ell)\Delta k_r(j\Delta r)}.$$

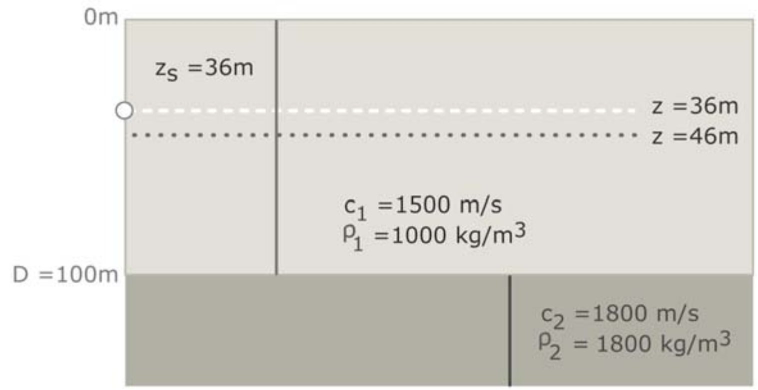

Example: Pekeris waveguide with pressure-release surface and penetrable fluid bottom

See Fig 4.5 in Jensen, Kuperman, Porter and Schmidt.
Computational Ocean Acoustics. New York: Springer-Verlag, 2000.

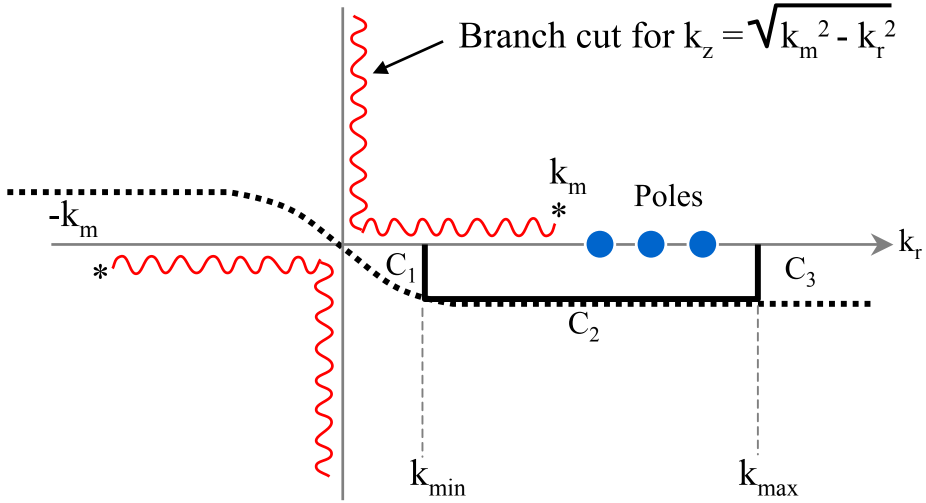

Complex integration contours for evaluation of wavenumber integral. The contour C2 is used for FFP integration, while the 'exact' hyperbolic tangent contour indicated by the dashed line is used for trapezoidal rule integration

Complex Contour Integration

$$
\begin{aligned}
g(r,z) &\simeq h(r) \int_C g(k_r,z)\, \sqrt{k_r}\, e^{ik_r r}\, dk_r\ , \\
&\simeq h(r) \int_{k_{\min}}^{k_{\max}} g(k_r - i\epsilon, z)\, \sqrt{k_r - i\epsilon}\ e^{i(k_r - i\epsilon)r}\, dk_r\ .
\end{aligned}
$$

Complex Contour Integration

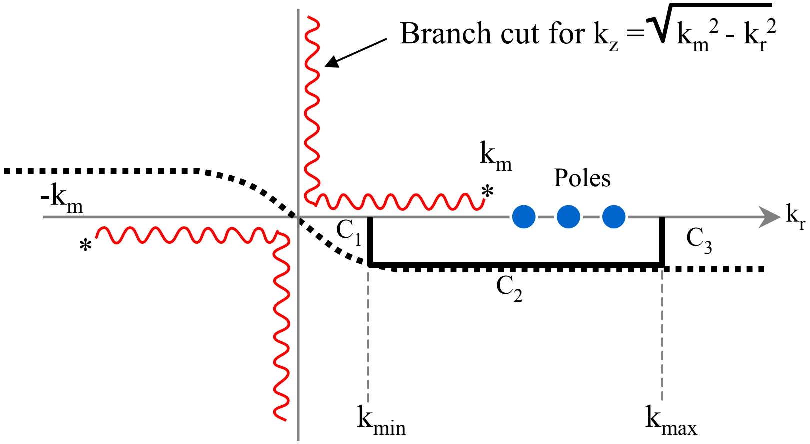

$$
\begin{aligned}
g(r,z) &\simeq h(r)\int_C g(k_r,z)\,\sqrt{k_r}\,e^{ik_r r}\,dk_r\,,\\
&\simeq h(r)\int_{k_{\min}}^{k_{\max}} g(k_r-i\epsilon,z)\,\sqrt{k_r-i\epsilon}\;e^{i(k_r-i\epsilon)r}\,dk_r\,.
\end{aligned}
$$

$$
\begin{aligned}
g(r,z)\,e^{-\epsilon r} &\simeq h(r)\,f(r,z)\,e^{-\epsilon r}\\
&= h(r)\int_{k_{\min}}^{k_{\max}} g(k_r-i\epsilon,z)\,\sqrt{k_r-i\epsilon}\;e^{ik_r r}\,dk_r\,.
\end{aligned}
$$

$$
\begin{aligned}
g^*(r_j,z)\,e^{-\epsilon r} &= h(r_j)e^{ik_{\min}r_j}f^*(r_j,z)\,e^{-\epsilon r}\\
&= h(r_j)\sum_{n=-\infty}^{\infty} f(r_j+nR,z)e^{-\epsilon(r_j+nR)}\\
&\simeq h(r_j)\Delta k_r e^{ik_{\min}r_j}\sum_{\ell=0}^{M-1}\left[g(k_\ell-i\epsilon,z)\,e^{ir_{\min}\ell\,\Delta k_r}\sqrt{k_\ell-i\epsilon}\right]e^{i\frac{2\pi\ell j}{M}}\,,
\end{aligned}
$$

$$
\begin{aligned}
g(r_j,z) &\simeq h(r_j)f(r_j,z)\\
&= e^{\epsilon r_j}h(r_j)\Delta k_r e^{ik_{\min}r_j}\sum_{\ell=0}^{M-1}\left[g(k_\ell-i\epsilon,z)\,e^{ir_{\min}\ell\Delta k_r}\sqrt{k_\ell-i\epsilon}\right]e^{i\frac{2\pi\ell j}{M}}\\
&\quad - h(r_j)\sum_{n\neq 0} f(r_j+nR,z)\,e^{-\epsilon nR}\,.
\end{aligned}
$$

$$
\epsilon = \frac{3}{R\log e} = \frac{3}{2\pi\,(M-1)\log e}\,(k_{\max}-k_{\min})\,,
$$

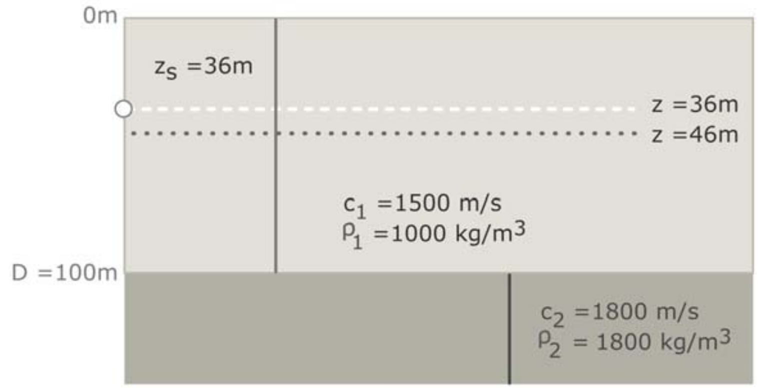

Example: Pekeris waveguide with pressure-release surface and penetrable fluid bottom

[See Jensen, Fig. 4.7]